# ANFIS Control based Improve System Performance and Power Quality for Grid Interfaced Solar WPS Using PMSM Drive

[1]K. Rama Asritha, [2]I. Balanjaneya Varma, [3]S. Jeetendra Srikar, [4]P. Samuel, [5]SK. Rinshad, [6]Mr. M.Sriramulu Naik

[1,2,3,4,5]B.Tech. Student, [6]Assistant Professor, EEE Department, Kallam Haranadhareddy Institute of Technology, Guntur (DT), Andhra Pradesh, India

**Abstract- Many high-performance industrial and traction PMSM drives do not need position sensors. This paper offers a solar photovoltaic array fed grid interfaced encoder-less permanent magnet synchronous motor (PMSM) based solar water pumping system due to the inconstancy of renewable energy sources. Regardless of solar insolation, the grid hookup assures a consistent water supply. Grids in developing and underdeveloped nations, on the other hand, have been shown to be inadequate. As a result, when the motor characteristics change, performance suffers significantly. Because of a hybrid multi-resonant generalised integrator-frequency locked loop (HMRGI-FLL) control structure, the SWP system can remain operational even when the grid is weak. The system's performance and power quality have been enhanced. Our field-oriented control techniques based on adaptive neuro-fuzzy inference systems are simple and versatile. Because of their distant position, such as grid radial ends, SWP systems are similarly prone to grid anomalies. The suggested structure rejects the DC-offset while keeping the lower order harmonic dominant. The HMRGI-FLL observer proposed in this study is based on an Adaptive Network-based Fuzzy Inference System (ANFIS), which replaces the traditional PI's adaptive model and process. A boost converter is a device that aids in the transmission of electricity on the grid. During a power outage, solar insolation regulates the output water flow. The PMSM's speed is controlled by sensor less vectors.**

**Keywords: ANFIS, neuro fuzzy, PMSM, Adaptive control, Power quality, sensor less control SWP, artificial intelligence, WPS, HMRGI-FLL, Utility grid.**

## I. INTRODUCTION

Permanent magnet synchronous motor (PMSM) drives have received a lot of attention in recent years due to various advantages such as low weight, high efficiency, power density, torque to inertia ratio, and so on. PMSM drives with vector control have a high dynamic performance and are commonly used in machine tools and electric vehicles. Accurate information about rotor speed and location is primarily required for indirect vector control of PMSM drives, which can be accomplished using position encoders or an estimator/observer. Sensorless PMSM management has piqued interest for a variety of reasons, including avoiding extra sensor costs, reducing hardware complexity, lowering maintenance requirements, and increasing the mechanical resilience and durability of the entire system [1]. Renewable energy sources (RES) have recently been found as a viable alternative to traditional energy sources in a number of applications. Water pumping is one of the possible sectors that uses a lot of fossil fuels, therefore using renewable energy for this application would minimise greenhouse gas emissions and carbon footprint [2]. Electric power production utilising solar photovoltaic (PV) is gaining acceptance due to its modular construction, reducing installation costs, and negligible operational costs [3]. Although a solar PV integrated water pumping system (WPS) is an option, the intermittent nature of solar energy limits its use to active hours, or when sunlight is available. This flaw must be fixed if WPS is to be used effectively. Some solutions to this problem include connecting the battery energy storage at the DC link, using pump storage, and using a fuel cell as a storage medium. However, these systems have drawbacks, including increased system complexity, cost, and space requirements [4-7]. Because the grid is an infinite source of energy, some current research suggests

 DOI : 10.35291/2454-9150.2022.0364 

integrating utility grid and solar water pumping (SWP) systems [8-10]. Integration with the power grid increases system utilisation while also increasing system dependability. [8] depicts a 1-utility grid-connected WPS with PFC that employs a boost DC-DC converter. The PFC converter maintains the UPF. [8, 9], and [11], Illustrate a 1- and 3-grid interactive WPS with a voltage source converter (VSC) on the grid side, respectively. State observer systems based on the Extended Kalman Filter (EKF), Extended Luenburger Observer (ELO), and Sliding Mode Observer, among others, have also been reported [5]-[6]. The majority of them are hampered by complicated calculation, sensitivity to parameter fluctuation, and the need for precise beginning conditions. The EKF has the advantage of simultaneously estimating parameters and speed by treating them as states. It is, however, computationally intensive and necessitates a high sampling frequency in order to apply a basic discrete-time equivalent model. When it comes to parameter variations, the sliding mode observer is basic and has low resilience. Sliding mode, on the other hand, is a discontinuous control with variable switching characteristics that can cause chattering and reduce control precision. Recently, adaptive estimating strategies based on Artificial Neural Networks (ANN) and Fuzzy Logic Control (FLC) have also been published [6]-[8]. The estimate accuracy, on the other hand, is dependent on the number of neurons and fuzzy membership functions used in the rule base and requires off-line tweaking. In the current literature, a quadrature signal generator based on a generalised integrator (GI) has been extensively documented for harmonic extraction [13-15]. A second order GI (SOGI) based structure is one of the simplest to apply among several harmonic extraction strategies due to its structural simplicity. It, on the other hand, has weak harmonics and DC-offset rejection capabilities. [14] and [17] present two improved topologies for DC-offset mitigation. Respectively, one has a dedicated loop to reject the DC-offset, while the other has two cascaded SOGIs. Despite the fact that the new structure is effective at rejecting DC offset, it is ineffective at mitigating dominant lower order harmonics. Although decreasing the filter's bandwidth improves harmonic rejection, it has an effect on dynamic response, and the system's steady state and dynamic performance must be constantly balanced. To address this issue, this study proposes a hybrid multi-resonant GI construction with multiple layers. The first layer is cascaded SOGI, which rejects the DC offset, while the subsequent layers aid in selective harmonic elimination (SHE) by adjusting filters to the specific harmonic component. As a result, as shown by the Bode plot in frequency domain analysis, the proposed control structure is capable of mitigating both DC-offset and dominating lower harmonics. A frequency locked loop (FLL) is used to make the system more tolerant of frequency variations. To validate the efficiency of the proposed control system, simulation experiments with various grid irregularities are used. In this study, the adaptation mechanism and adaptive model of the traditional stator current error HMRGI-FLL are replaced with a non-linear adaptive ANFIS controller, resulting in a novel ANFIS-based HMRGI-FLL technique. Figure 2 depicts the proposed ANFIS HMRGI-FLL sensor less configuration. The ANFIS architecture has well-known advantages for modelling a highly nonlinear system because it combines fuzzy reasoning's ability to handle uncertainty with ANN's ability to learn from processes [15]. As a result, the ANFIS is used to create an adaptive model of variable speed PMSM under extremely uncertain operating conditions, which automatically adjusts for changes in parameters such as inductance, resistance, and so on. The ANFIS architecture was adjusted on the fly using an error gradient-based dynamic back propagation approach. The proposed system is modelled in MATLAB/Simulink. Under variable speed PMSM operation, a full comparison based on modelling and experimental findings is also presented for both ANFIS and sliding mode observers. Furthermore, a simulation and experimental investigation is carried out for various PMSM resistance and inductance values in order to test the proposed algorithm's resilience to parameter fluctuation.

The following are the key characteristics of the study provided.

- A hybrid multi-resonant generalised integrator-frequency locked loop (HMRGI-FLL) control structure is used to filter the abnormal grid voltage and extract its fundamental component.
- The SWP system is linked to the single-phase utility grid, allowing for continuous water pumping regardless of available solar insolation.
- PQ concerns such as voltage sag, voltage swell, grid current distortion, and grid voltage distortion are reduced, allowing the described system to comply with the IEEE standard for PQ in grid-connected systems [22].
- To manage the speed of the PMSM, a sensor-less vector control approach is used, which improves system dependability and reduces system costs.

## II. SYSTEM ARCHITECTURE

The system layout of a grid-integrated SWP system with a PMSM drive is depicted in Figure 1. This system includes a solar PV array, a boost converter for maximum power point tracking (MPPT), a voltage source inverter (VSI) to drive the motor, another boost front end converter

 DOI : 10.35291/2454-9150.2022.0364 

(FEC), and a PMSM linked to a pump. A sensor-less vector control approach is used to control the speed of the PMSM. An incremental conductance (INC) method is used for MPPT by changing the duty ratio of switch Sb [7]. The grid powers the DC connection via an FEC converter. Proper SFEC switch switching allows electricity to flow from the grid. An RC filter (Rf, Cf) and an interface inductor are used to remove switching harmonics and current ripples (Lf). The performance of WPS is validated under various operating conditions through experimental examination on a laboratory-developed system.

## III. SYSTEM OPERATION AND CONTROL

The planned SWP system has two modes of operation. The first mode is the grid linked mode, which is activated when the utility grid is available. When the grid is inaccessible, the standalone mode is activated. When the SWP system is connected to the grid, the pump's speed is reduced to the nominal speed, and the excess electricity generated by the solar PV array is fed into the grid. To keep the WPS operational even in poor grid conditions, an HMRGI-FLL-based framework is used. The HMRGI-FLL structure isolates the fundamental component from dirty grid voltage and uses it to generate unit templates. The unit template is multiplied by the weight component to generate sinusoidal reference grid current. The FEC is turned on and off in response to the reference grid current, ensuring that the grid current remains sinusoidal. When the power goes out, the pump speed adjusts to compensate for the change in solar insolation. For control, the WPS is divided into three sections. The first method is to regulate MPPT using the INC MPPT algorithm. The second method, as shown in Fig. 2, is to use sensor-less vector control to regulate the speed of the PMSM. A stationary stator flux observer-based technique is used to determine speed and location. The third option is to control the flow of power through the utility grid. This is accomplished by employing an HMRGI-FLL-based control strategy.

*A. MPPT:*

One of the most often utilised MPPT techniques is the INC algorithm. The duty ratio is controlled by the MPPT algorithm such that the instantaneous and incremental conductance's are equal. Even in constantly changing environmental circumstances, it allows for quick MPP tracking [9].

*B. Rotor Speed and Position Estimation:*

PMSM location as well as speed information are required for PMSM speed control. Although an encoder may readily provide these details, their usage for submersible water pumping is not suggested owing to the complexity and expense required. The introduction of encoders has resulted in major dependability concerns due to the hostile environment in which submersible pumps operate. Long cables are used to transfer high frequency low amplitude encoder signals from the encoder to the controller, polluting them and limiting them to surface water pumping. As a result, for PMSM speed management, we employ a stationary flux observer-based rotor position and speed estimate using SOGI-FLL, as described in [19] for sensor less operation of an induction motor. The back emf in stationary reference frame (es, es) of a PMSM is given as,

$$e_{s\alpha} = v_\alpha - R_s * i_\alpha, \quad e_{s\beta} = v_\beta - R_s * i_\beta \qquad (1)$$

where, (vα, vβ) and (iα, iβ) are the stationary reference frame voltages and currents, respectively, and Rs is the stator winding resistance.

SOGI-FLL structure is used to estimate the stationery components of stator flux (ψα, ψβ). The SOGI-FLL structure's output is denoted as [23],

$$\psi_{\alpha\beta} = \frac{K\omega_{mest}}{S^2 + K\omega_{mest}S + \omega_{mest}^2} * e_{s\alpha\beta} \qquad (2)$$

where ωmest is the estimated electrical frequency in radians per second. The resulting flux linkage (ψs) is computed as follows:

mest is the estimated electrical frequency in rad/sec. The resultant flux linkage (ψs) is calculated as,

$$\psi_s = \sqrt{\psi_\alpha^2 + \psi_\beta^2} \qquad (3)$$

The estimated electrical position (θest) is expressed as,

$$\theta_{est} = \tan^{-1}\left[\frac{\psi_\beta}{\psi_\alpha}\right] \qquad (4)$$

The estimated rotor speed (ωmest) is calculated as,

$$\omega_{mest} = \frac{1}{P}\frac{d}{dt}(\theta_{est}) = \frac{\psi_\alpha . \dot{\psi}_\beta - \psi_\beta . \dot{\psi}_a}{P\psi_s^2} \qquad (5)$$

where p denotes the number of pole pairs,ψα is the derivative of ψα and ψβ is the derivative of ψβ. Because of the WPS's grid integration, the following scenarios can be visualized: I the grid is operational, and (ii) the grid has failed. When the grid is available (i.e. Vt ≥ Vth), the pump is normally operated at its nominal values, and the boost FEC regulates the DC link voltage. During grid failure (i.e. Vt < Vth), however, the DC link voltage (Vdc) is controlled by an islanded Vdc controller and is expressed as,

 DOI : 10.35291/2454-9150.2022.0364 

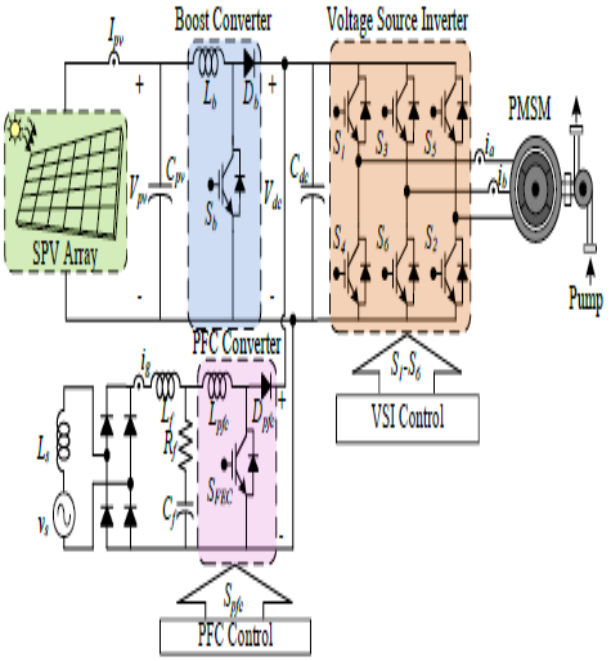


**Fig. 1 System Configuration**

$$\omega_{ref} = \left( K_{pidc} + \frac{K_{iidc}}{S} \right) \{ V_{dcref}(k) - V_{dc}(k) \} \qquad (6)$$

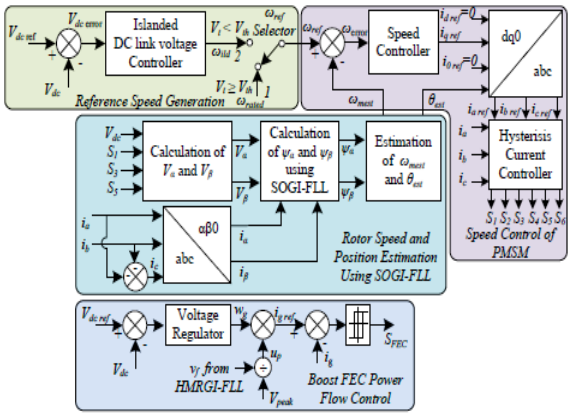


**Fig.2 depicts the proposed SWP system's control scheme.**

where, Kpidc and Kiidc Kpidc are the proportional and integral gains of the islanded Vdc controller, respectively. Vth is chosen to be 70% of Vt. The speed controller governs the PMSM's speed. The speed controller receives the error generated by comparing ref and mest. Its output is referred to as reference quadrature axis current (iq ref), which is denoted as

$$i_{q\,ref}(k) = \left( K_{p\omega} + \frac{K_{i\omega}}{S} \right) \{ \omega_{ref}(K) - \omega_{mest}(K) \} \qquad (7)$$

where, Kpω and Kiω denote the controller gains

The pump speed is limited to its rated value during SWP operation. As a result, the direct axis reference current (id ref) is set to zero. The inverse Park's transform is used to obtain the PMSM reference currents ia ref, ib ref, and ic ref from id ref and iq ref. The gating pulses (S1-S6) are generated by using a hysteresis controller to compare the reference and sensed motor currents (ia, ib, and ic).

C. Control of Grid Power Flow

The control technique depicted in Fig. 2 is used to visualise the control of grid power flow. The voltage regulator controls Vdc during grid availability by feeding it the error of reference and sensed Vdc. The weight component (wg) of the voltage regulator output is expressed as.

$$w_g(K) = \left( K_{pdc} + \frac{K_{idc}}{S} \right) \{ V_{dcref}(k) - V_{dc}(k) \} \qquad (8)$$

where Kpdc and Kidc are the voltage regulator's proportional and integral gains.

Grid voltage filtering is accomplished using the HMRGI-FLL control structure depicted in Fig. 3. Even under abnormal grid conditions, it rejects harmonics and DC-offset in the grid voltage and generates a fundamental frequency unit template (up).

The "Up" expression is expressed as, $u_p = |v_f| / V_{peak}$ (9)

Where $|V_f|$, is the magnitude of fundamental grid voltage (vf) and Vpeak is the peak grid voltage (Vpeak) expressed as,

$$V_{peak} = \sqrt{v_f^2 + q v_f^2} \qquad (10)$$

The reference grid current (igref) is the product of wg as well as unit template (up) and it is represented as,

$$i_{gref} = w_g * u_p \qquad (11)$$

The difference between igref and sensed grid current (ig) is used to generate the FEC switching signal, as shown in Fig. 2.

## IV. HMRGI-FLL ANALYSIS

The grid voltage is initially filtered using the suggested HMRGI-FLL structure shown in Fig. 3 to ensure proper operation even in abnormal grid situations. The HMRGI-FLL control framework is made up of several layers. The first layer is cascaded SOGI (CSOGI), which rejects DC-offset and provides band pass filtering, while the subsequent layers enable, SHE by adjusting filters to the specific harmonic component. Because the 3rd, 5th, and 7th harmonics are the primary harmonic components in a 1-system, they are filtered by SHE filters and removed using a harmonic decoupling network. As a result, the proposed control structure provides better filtering and may reduce both DC-offset and dominating lower harmonics. The transfer function (TF) for SOGI is given in [17].

 DOI : 10.35291/2454-9150.2022.0364 

$$D_{SOGI} = \frac{v_f(s)}{v(s)} = \frac{k\omega' s}{S^2 + k\omega' s + \omega'^2} \qquad (12)$$

$$Q_{SOGI} = \frac{qv_f(s)}{v(s)} = \frac{k\omega'^2}{S^2 + k\omega' s + \omega'^2} \qquad (13)$$

where'ω' denotes the grid frequency and k = 2ζ, ζ denotes the damping factor The value of ζ controls the settling time ts.

The ts is written as,

$$t_s = 4/(\zeta\omega^1) \qquad (14)$$

\'ζ value is between 0 and 1.

[21] is the TF for CSOGI.

$$D_{CSOGI} = \frac{v_f(s)}{v(s)} = \frac{c_1 c_2 \omega'^2 s^2}{(s^2 + c_2\omega' s + \omega'^2)(s^2 + \omega'^2) + c_1 c_2 \omega'^2 s^2} \qquad (15)$$

$$Q_{CSOGI} = \frac{qv_f(s)}{v_s(s)} = \frac{c_1 c_2 \omega'^3 s}{(s^2 + c_2\omega' s + \omega'^2)(s^2 + \omega'^2) + c_1 c_2 \omega'^2 s^2} \qquad (16)$$

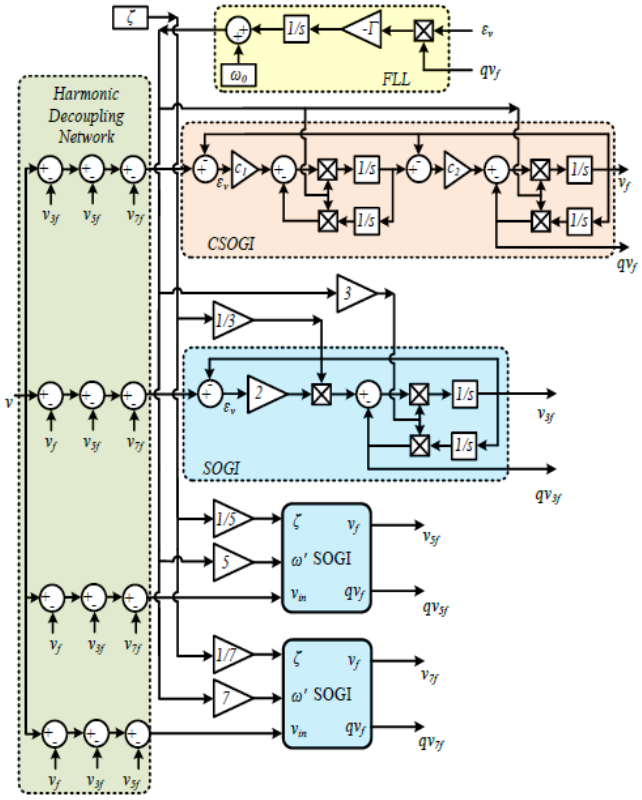


**Fig. 3 Structure of HMRGI-FLL**

For in-phase and quadrature components, the HMRGI-FLL TFs are in [15]. The frequency domain analysis of HMRGI-performance FLL's shows that it efficiently filters the fundamental frequency component while rejecting all other frequency components. The frequency plot for in-phase and quadrature components demonstrates that the provided structure, in addition to DC-offset rejection, can efficiently remove dominant 3rd, 5th, and 7th harmonic components via SHE.

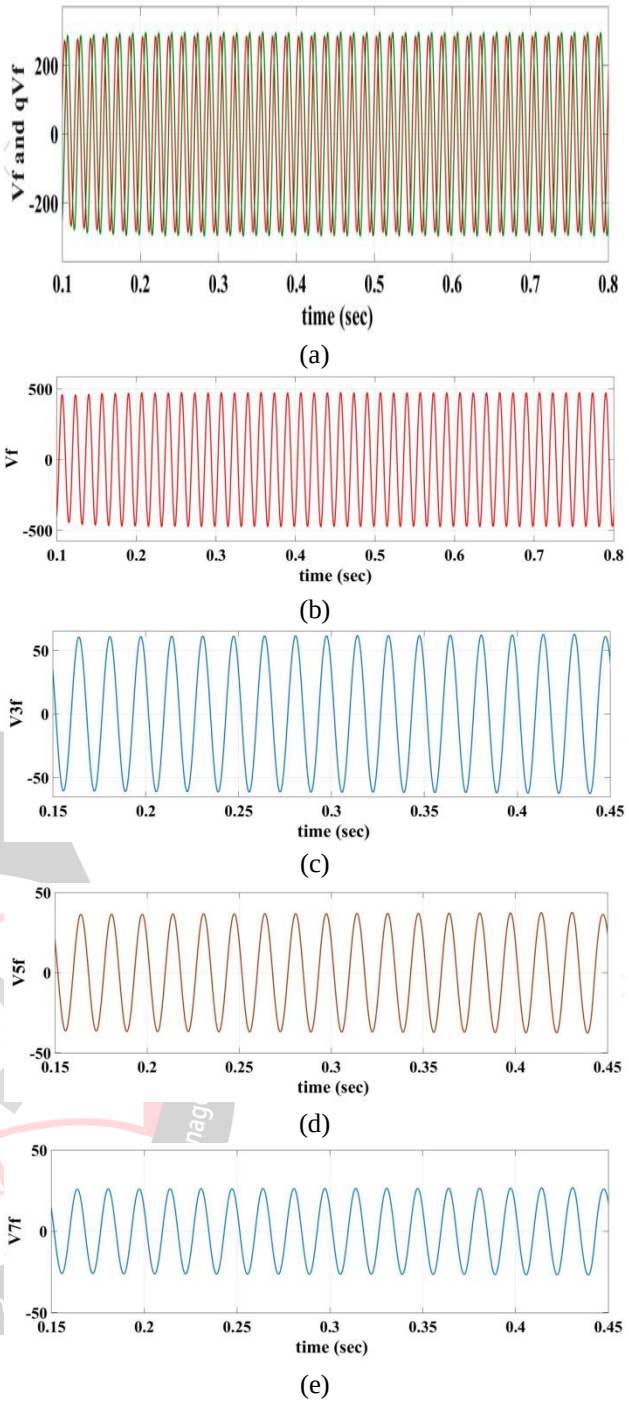


**Fig.4 shows the in-phase and quadrature fundamental and harmonic voltage extraction capability of the HMRGI-FLL (a-e).**

Figure 4 depicts the ability of FLLs with HMRGI capability to extract fundamental and harmonic voltages in phase and quadrature (a-e). The results show that each layer of the HMRGI-FLL successfully extracts the frequency in-phase and quadrature components. The harmonic decoupling network decouples the major harmonic component and thus performs the SHE functions. The CSOGI structure successfully rejects the DC-offset and higher order frequency components, leaving only the basic in-phase component (vf) and quadrature phase component (qvf) to be recovered from contaminated grid voltage.

 DOI : 10.35291/2454-9150.2022.0364 

## V. RESULTS AND DISCUSSION

*A. When the grid is unavailable, the performance remains stable.*

When the grid is unavailable, the ωm est is a function of available PV array power. In this case, the array voltage (Vpv) and current (Ipv) settle at their MPP, as shown in Fig. 5. (a-d).

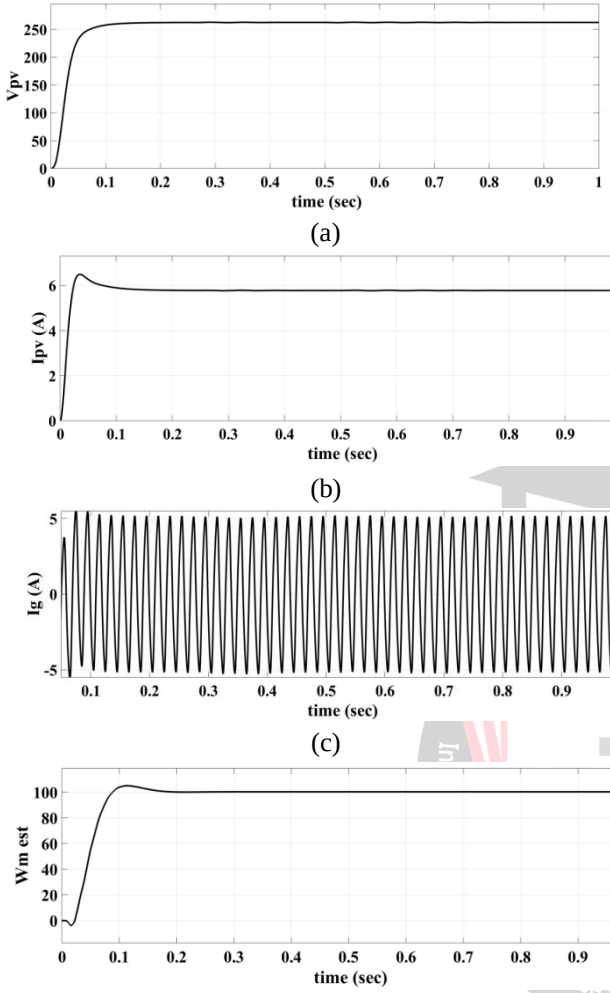


**Fig. 5 Initial SWP system performance when (a) solar insolation is 1000W/m2 and the grid is available.**

*B. Performance during Insolation Change*

Figures 6 (a-d) and 6 (e-h) show the performance of WPS in grid linked and standalone mode for insolation change, respectively. The pump speed remains constant when the system is connected to the grid, but it varies with the change in insolation when the system is not connected to the grid, as shown in Fig. 6.

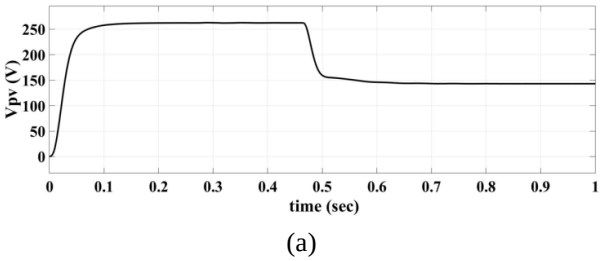


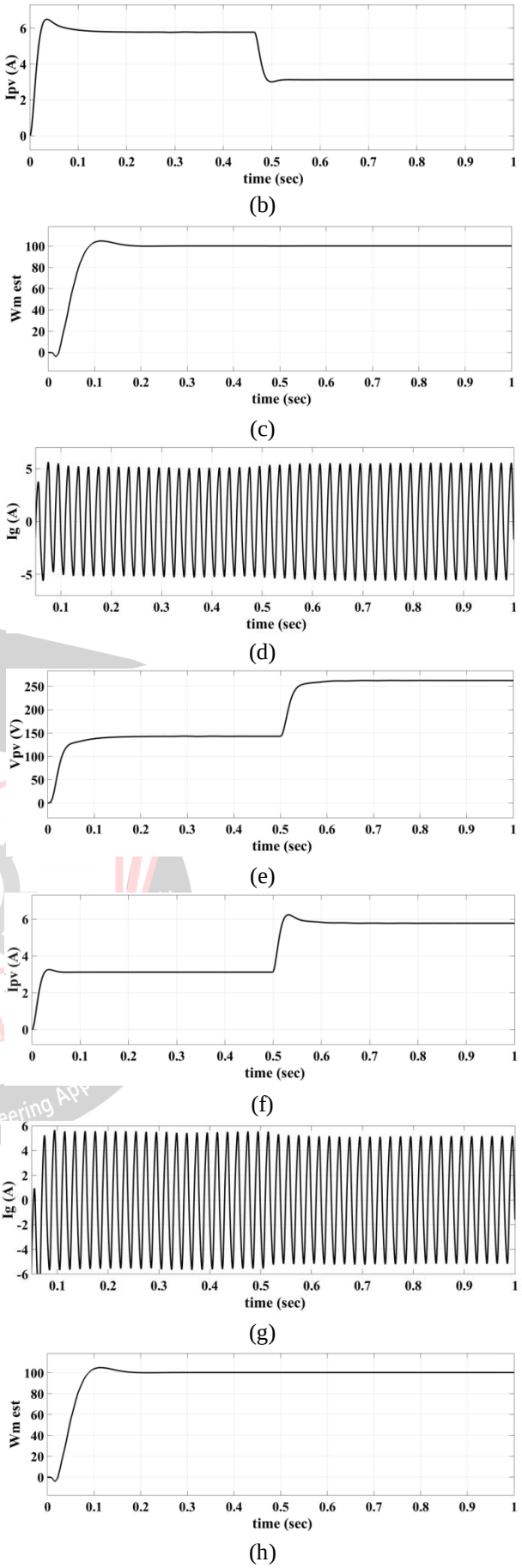


**Fig. 6 shows the dynamic performance of an SWP system during standalone operation when the solar insolation changes from 1000W/m2 to 500W/m2 and vice versa.**

 DOI : 10.35291/2454-9150.2022.0364 

*C. Dynamic Performance during Grid Availability*

In grid-tied mode, insolation changes have no effect on the ωm est. As solar insolation drops from 1000W/m2 to 500W/m2, the utility grid supplies the remaining power needed to run the PMSM at rated speed, as shown in Figs. 7 and 8. (a-d). The pump is powered by the utility grid when solar PV energy is not available at night. In this case, the grid supplies all of the energy needed to run the PMSM, and Ipv is zero, as shown in Figures 7 and 8. (e-h). This improves the efficiency with which the system is used.

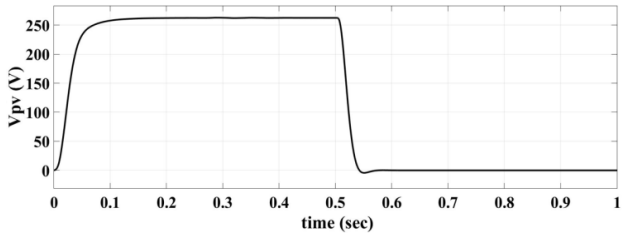


(a)

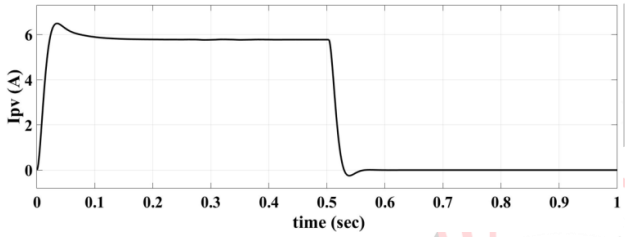


(b)

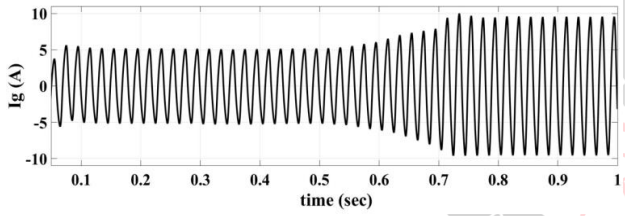


(c)

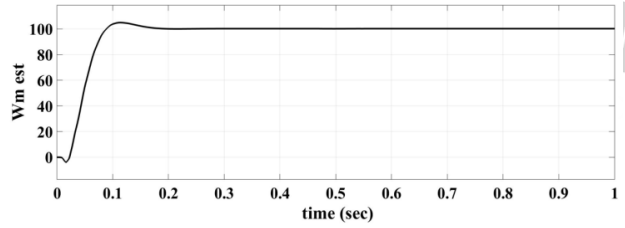


(d)

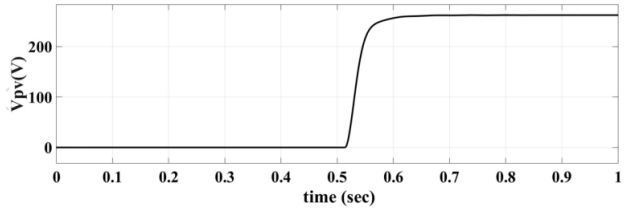


(e)

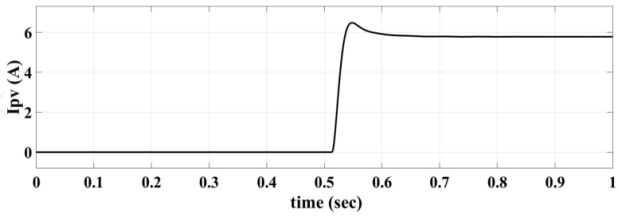


(f)

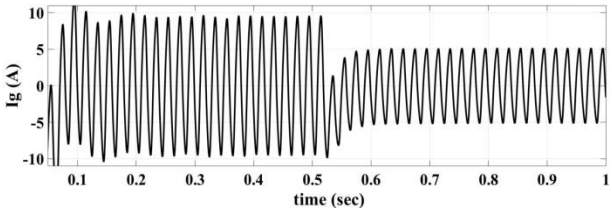


(g)

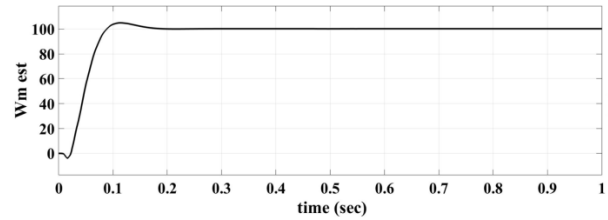


(h)

**Fig. 7 Dynamic performance of SWP system during grid connected operation when (a-d) Solar insolation changes from 1000W/m2 to 0W/m2 and (e-h) Solar insolation changes from 0W/m2 to 1000W/m2**

## VI. PROPOSED CONTROL TECHNIQUE

*A. HMRGI-FLL -ANFIS position and speed observer*

In recent years, neuro fuzzy synergisms for modelling and adaptive control of nonlinear systems have improved. The heart of neuro-fuzzy synergisms is a shared framework known as adaptive networks, which integrates both neural networks and fuzzy models. The name of the fuzzy model that operates within the framework of adaptive networks is Adaptive-Network-based Fuzzy Inference System (ANFIS). ANFIS's advantages include fast convergence due to hybrid learning and the ability to modify the form of input membership functions. As a result, in terms of tracking and adaptability, it outperforms all other controllers. The ANFIS, as demonstrated in [19, 20], can generate a highly nonlinear mapping, making it superior to standard linear approaches and having some advantages over neural networks. Because the PMSM drive system is highly nonlinear and operates under dynamic conditions, estimating the precise value of back-EMF, which also conveys information about rotor position and speed, is especially difficult. To address this issue, an ANFIS-based dynamic model of PMSM is being developed. For ANFIS training, a detailed mathematical model of the plant is not required. To create an adaptive model, all that is needed is the system's order as well as enough input/output data from the real plant [18]. Simultaneously, the goal output from the real plant is compared to the output of the ANFIS-based dynamic model, and the weights are updated based on the difference. In the proposed work, the dynamic

 DOI : 10.35291/2454-9150.2022.0364 

model is constantly modified by forcing its predicted currents to match the actual currents of the PMSM using an ANFIS structure with a dynamic back propagation approach. Regardless of parameter fluctuations or external disruptions, the adaptive model accurately replicates the real model once the predicted currents are identical to the actual currents.

**Layers**

In this layer, which is also known as the fuzzification layer, each node is represented by a square. Each input is assigned one of three fuzzy membership functions. The trapezoidal and triangular membership functions, as shown in Fig. 5, are used to reduce computing costs, and their associated node equations are as follows:

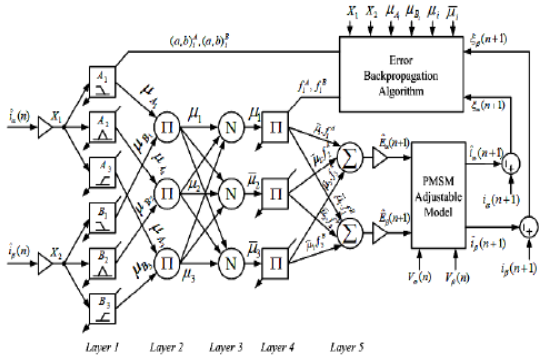


**Fig. 8 Proposed ANFIS architecture.**

$$\mu A_1(X_\alpha) = \mu\beta_1(X_\beta) = \begin{cases} 1 & X \le b_1 \\ \frac{X-a_1}{b_1-a_1} & b_1 < X < a_1 \\ 0 & X \ge a_1 \end{cases} \quad (17)$$

$$\mu A_2(X_\alpha) = \mu\beta_2(X_\beta) = \left\{1 - \frac{X-a_2}{0.5b_2} |X - a_2| \le 0.5b_2\right\}$$

(18)

$$0 \quad |X - a_2| \ge 0.5b_2$$

$$\mu A_3(X_\alpha) = \mu\beta_3(X_\beta) = \begin{cases} 0 & X \le b_3 \\ \frac{X-a_3}{b_3-a_3} & a_3 < X < a_3 \\ 1 & X \ge b_3 \end{cases} \quad (19)$$

In response to the error, the linguistic value of each membership function is generated by changing the values of parameters ai, bi. The parameters of this layer are known as assumption parameters or causal parameters.

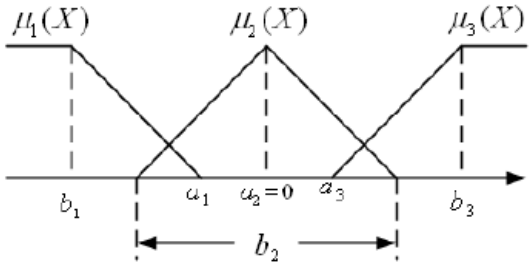


**Fig. 9 Fuzzy membership functions**

**Layer 1:** Each node in this layer is a circle labelled as that π which multiplies incoming signals and sends them to the next layer.

$$\mu_i = \mu_{A_i}(X_\alpha)\mu_{B_i}(X_\beta) \quad i = 1, 2, 3$$

Each node's output represents the firing strength of a rule in this case.

**Layer 2:** In this layer, each node is represented by a circle. This layer determines the normalised firing strength of each rule as follows:

$$\bar{\mu}_i = \frac{\mu_i}{\mu_1 + \mu_2 + \mu_3} \quad i = 1, 2, 3$$

**Layer 3:** consists of square nodes with the following node functions:

$$O_i = \bar{\mu}_i f_i^j = \bar{\mu}_i(a_0^i + a_1^i . X_j), \quad i = 1, 2, 3$$
$$j = \alpha, \beta$$

parameters that follow.

**Layer 4:** Also known as the output layer, this layer computes the following output:

$$Y_1 = \bar{\mu}_1 f_1^A + \bar{\mu}_2 f_2^A + \bar{\mu}_3 f_3^A$$
$$Y_2 = \bar{\mu}_1 f_1^B + \bar{\mu}_2 f_2^B + \bar{\mu}_3 f_3^B$$

This layer's output is now multiplied by the normalizing factor and passed through the low pass filter to determine the estimated value of the back -EMF's $\hat{E}_\alpha$ and $\hat{E}_\beta$.

## CONCLUSION

This paper proposes an ANFIS-HMRGI-FLL based PMSM speed and position estimation method that is particularly useful in low-speed operating environments. HMRGI-FLL offers simple implementation and processing, whereas ANFIS non-linear modelling offers parameter fluctuation immunity. The improved FEC converter improved PQ at the grid terminals while increasing grid power flow. Despite the distorted grid voltage, ANFIS has eliminated grid current distortion and kept current THD below the allowable limits. The grid indices correspond to the IEEE-519 and IEEE-1564 performance criteria for PQ performance. Even in the face of grid anomalies such as grid voltage sag, grid voltage swell, and grid voltage distortion, the WPS performs effectively. The system's cost is reduced by removing the speed sensor. A systematic ANFIS structure is presented in order to develop a dynamic model of PMSM that does not require an explicit mathematical model of the plant and compensates for parameter changes automatically. An on-line weight tuning strategy is developed using the dynamic error back propagation method to build an adaptive model under a variety of operating conditions. In addition, the ANFIS is built around the stator current. Under variable torque and speed PMSM operation with parameter adjustment, the recommended approach accurately estimates position and speed.

## REFERENCES

[1] P. P. Acarnley and J. F. Watson, "Review of position-sensorless operation of brushless permanent-magnet machines," IEEE Trans. onIndustrial Electronics, vol. 53, no. 2, pp. 352-362, April 2006.

 DOI : 10.35291/2454-9150.2022.0364 

[2] S. Murshid and B. Singh, "Implementation of PMSM drive for a solar water pumping system," IEEE Trans. Ind. Appl., vol. 55, no. 5, pp. 4956-4964, Sept.-Oct. 2019.

[3] S. Jain, R. Karampuri and V. T. Somasekhar, "An integrated control algorithm for a single-stage PV pumping system using an open-end winding induction motor," IEEE Trans. Ind. Elect., vol. 63, no. 2, pp. 956-965, 2016.

[4] A. Khiareddine, C. Ben Salah and M. F. Mimouni, "Strategy of energy control in PVP/battery water pumping system," in Proc. International Conf. on Green Energy, Sfax, 2014, pp. 49-54.

[5] P. García, C. A. García, L. M. Fernández, F. Llorens and F. Jurado, "ANFIS-based control of a grid-connected hybrid system integrating renewable energies, hydrogen and batteries," IEEE Trans. Ind. Info., vol. 10, no. 2, pp. 1107-1117, May 2014.

[6] I. Ducar and C. Marinescu, "Increasing the efficiency of motor-pump systems using a vector controlled drive for PMSM application," in proc. Int. Symp. on Fund. of Electrical Engg. (ISFEE), Bucharest, 2014, pp. 1-5.

[7] A. B. C. S. B. Slama and A. Chrif, "Efficient design of a hybrid (pv-fc) water pumping system with separate mppt control algorithm," lJCSNS Int. J. of Comp. Science and Net. Security, vol.12, pp. 53-60, January 2012.

[8] S. Murshid and B. Singh, "Utility grid interfaced solar water pumping system using PMSM drive," in proc. IEEE Int. Conf. on Pow. Elect., Drives and Energy Syst. (PEDES), Chennai, India, pp. 1-6, 2018.

[9] R. Kumar and B. Singh, "Grid interactive solar PV-based water pumping using BLDC motor drive," IEEE Trans. Ind. Appl., vol. 55, no. 5, pp. 5153-5165, Sept.-Oct. 2019.

[10] B. Singh and S. Murshid, "A grid-interactive permanent magnet synchronous motor driven solar water-pumping system," IEEE Trans. Ind. Appl., vol. 54, no. 5, pp. 5549-5561, Sept.-Oct. 2018.

[11] S. Murshid and B. Singh, "A multi-objective GI based control for effective operation of PV pumping system under abnormal grid conditions," IEEE Trans. Ind. Info. [Early Access]

[12] S. Gude and C. Chu, "Dynamic performance enhancement of single-phase and two-phase enhanced phase-locked loops by using in-loop multiple delayed signal cancellation filters," IEEE Trans. Ind. Appl. [Early Access]

[13] T. R. Oliveira, W. W. A. G. Silva, S. I. Seleme and P. F. Donoso-Garcia, "PLL-based feed-forward control to attenuate low-frequency common-mode voltages in transformerless LVDC systems," IEEE Trans. Ind. Appl., vol. 55, no. 3, pp. 3151-3159, May-June 2019.

[14] S. Sahoo, S. Prakash and S. Mishra, "Power quality improvement of grid-connected DC microgrids using repetitive learning-based PLL under abnormal grid conditions," IEEE Trans. Ind. Appl., vol. 54, no. 1, pp. 82-90, Jan.-Feb. 2018.

[15] S. Gude and C. Chu, "Single-phase enhanced phase-locked loops based on multiple delayed signal cancellation filters for micro-grid applications," IEEE Trans. Ind. Appl.

[16] Q. Huang and K. Rajashekara, "An improved delayed signal cancellation PLL for fast grid synchronization under distorted and unbalanced grid condition," IEEE Trans. Ind. Appl., vol. 53, no. 5, pp. 4985-4997, Sept.-Oct. 2017.

[17] D. Yazdani, A. Bakhshai and P. K. Jain, "A three-phase adaptive notch filter-based approach to harmonic/reactive current extraction and harmonic decomposition," IEEE Trans. Pow. Elect., vol. 25, no. 4, pp. 914-923, April 2010.

[18] J.-S. R. Jang, "ANFIS: Adaptive-network-based fuzzy inference system," IEEE Trans. on Systems, Man and Cybernetics, vol. 23, no. 3, pp. 665-684, May 1993.

[19] J.-S. R. Jang and C.-T. Sun, "Neuro-fuzzy modeling and control," Proc. of the IEEE, vol. 83, no. 3, pp. 378-406, March 1995.

[20] J.-S. R. Jang, "Self-learning fuzzy controllers based on temporal back propagation," IEEE Trans. on Neural Networks, vol. 3, no. 5, pp. 714-723, Sept. 1992.

## AUTHORS PROFILE

K. Rama Asritha is an Under Graduate student studying IV B.Tech Electrical and Electronics Engineering from Kallam Haranadhareddy Institute of Engineering & Technology, Guntur, A.P, India. His research interests include Powe Electronics and Electrical Machines.

I. Balanjaneya Varma is an Under Graduate student studying IV B.Tech Electrical and Electronics Engineering from Kallam Haranadhareddy Institute of Engineering & Technology, Guntur, A.P, India. His research interests include Power Electronics and Electrical Machines.

S. Jeetendra Srikar is an Under Graduate student studying IV B.Tech Electrical and Electronics Engineering from Kallam Haranadhareddy Institute of Engineering & Technology, Guntur, A.P, India. His research interests include Power Electronics and Electrical Machines.

P. Samuel is an Under Graduate student studying IV B.Tech Electrical and Electronics Engineering from Kallam Haranadhareddy Institute of Engineering & Technology, Guntur, A.P, India. Her research interests include Power Electronics and Electrical Machines.

SK. Rinshad is an Under Graduate student studying IV B.Tech Electrical and Electronics Engineering from Kallam Haranadhareddy Institute of Engineering & Technology, Guntur, A.P, India. Her research interests include Power Electronics and Electrical Machines.

Mr. M.Sriramulu Naik received his B. Tech degree In Electrical & Electronics Engineering from Acharya Nagarjuna University in 2007 and He Completed his Master of Technology in Power Electonics & Electrical Drives from JNTU Kakinada in 2011,Andhra Pradesh,India. He is having 10 years of teaching experience and pursuring Ph.D. in Acharya Nagarjuna University.currently he is an Assistant Professor in the Department of E.E.E., Kallam Haranadhareddy Institute of Technology, Guntur, India. His Research area of interests includes Power Electronics,Drives,FACTS Devices.

 DOI : 10.35291/2454-9150.2022.0364 